http://www.sjst.psu.ac.th

Original Article

Experimental and numerical investigation of dam break flow propagation passed through complex obstacles using LES model based on FVM and LBM

Chartchay Chumchan and Phadungsak Rattanadecho*

*Department of Mechanical Engineering, Faculty of Engineering,
Thammasat University, Rangsit Campus, Khlong Luang, Pathumthani, 12120 Thailand*

Abstract

Dam break analysis plays a key role in hydraulics engineering for safety. In this paper, 3D numerical simulations of dam-break flow using Finite Volume and Lattice Boltzmann methods are studied and discussed. All the computation in this work is achieved by ANSYS Fluent and XFlow. Large Eddy Simulation (LES) is employed as the turbulence model and the free surface flow is captured using a Volume of Fluid (VOF) model in the two simulation approaches. Results are then compared with experimental data on dam-break flow through complex obstacles. This experimental data is obtained by a high-speed camera aiming to capture free surface waves. The comparison between the experimental data and simulations shows good tendency. However, LBM requires less computational time.

Keywords: dam-break, Volume of Fluid (VOF), Finite Volume Method (FVM), Lattice Boltzmann Method (LBM), Large-eddy simulation (LES)

1. Introduction

A dam and dike break event damage can occurred due to a variety of reasons such as overtopping, foundation defects, piping, seepage, earthquake, etc. (Alhasan, Jandora, & Říha, 2015; Marsooli & Wu, 2014; Tayfur & Guney, 2013). Usually, the dam-break flows propagate over complex topography that include land, building, bridge piers, and roadway that can cause morphodynamical problems. For risk assessment purposes, therefore, it is of great importance to predict the flows mechanism after dam or dike break that serious damage settlements and the environment.

Recently, morphodynamical model of fast geo-morphic processes and more complex morphodynamical multi-layers and multi-phase models were proposed that account for the mass and momentum conservation for both water and sediments also in the presence of obstacles (Di Cristo *et al.*, 2018; Evangelista, Altinakar, Di Cristo, & Leopardi, 2013; Evangelista, Giovinco, & Kocaman, 2017;

Evangelista, Greco, Iervolino, Leopardi, & Vacca, 2015; Evangelista, 2015; Onda, Hosoda, Jaćimović, & Kimura, 2018; Syvitski *et al.*, 2009). Furthermore, considerable amount of research has recently concerned modeling of flood propagation processes, which makes more challenging predicting the wave front propagation and celerity. The Concerted Action on Dam-break Modelling (CADAM) project provided the variety of techniques and approaches to promote the comparison of numerical dam break models and modeling procedures with analytical, experimental and field data (Morris, 1999).

Investigation of Extreme Flood Processes & Uncertainty (IMPACT) project was to identify and emphasize the uncertainty associated with the various components of the flood prediction process (IMPACT, 2004). A set of experimental data was measured by Soares-Frazão & Zech (2007) and Frazão, Noël, & Zech (2004) and then was used for validation of numerical models within IMPACT project to predict dam-break flow through a single obstacle. In addition, the same author published experimental data for dam-break flow through multi-obstacles in the following year (Soares-Frazão & Zech, 2008).

*Corresponding author
Email address: ratphadu@engr.tu.ac.th

Due to high cost of field and laboratory experiments, the numerical simulation becomes an attractive topic and cost-effective. One- and two-dimensional models of shallow water equations (SWEs) are usually applied to the model of dam break flows. However, these models are limited in their ability to capture the flood spatial extent, in terms of flow depth (Biscarini, Francesco, & Manciola, 2010). Therefore, all details of flow propagation must be investigated by three-dimensional models. Generally, the 3D Navier-Stoke (NS) equations are solved by using Finite Volume Method (FVM) but this method has a major disadvantage as the meshing process is time consuming.

The Lattice Boltzmann Method (LBM) is an alternative numerical fluid dynamics scheme based on Boltzmann's kinetic equation. The LBM recovers the NS equations by using the Chapman-Enskog expansion in such a way that velocity and pressure are computed as momentum of the distribution function (Mohamad, 2011). Furthermore, the LBM is a statistical approach that provides simple implementation, computational efficiency, and an ability to represent complex geometries via the use of cubic lattice structure (Biscarini, Di Francesco, Nardi, & Manciola, 2013; Xu & He, 2003). Additionally, Smoothed Particle Hydrodynamics (SPH) is a meshfree particle method based on Lagrangian formulation, and has been widely applied to different areas in engineering and science (Kajzer, Pozorski, & Szewc, 2014; Liu & Liu, 2010; Monaghan, 1992) and to simulate free surface flow is dam-break problem (Albano, Sole, Mirauda, & Adamowski, 2016; Jian, Liang, Shao, Chen, & Yang 2016; Kao & Chang, 2012; Xu, 2016). However, SPH is undeniably computational expensive (Dickenson, 2009).

In order to model the dam break flows on a numerical models with grid based methods, the Volume of Fluid (VOF) is used, which is one of best-known methods for tracking the free surface flows (Hirt & Nichols, 1981). Generally, the 3D free surface modeling of the VOF and RANS models are widely applied to model dam break event (Marsooli & Wu, 2014; Robb & Vasquez, 2015; Yang, Lin, Jiang, & Liu, 2010) with results in good agreement. However, the Large Eddy Simulation (LES) turbulence model coupled with VOF can better capture the fluctuation of the free surface and velocity (LaRocque, Imran, & Chaudhry, 2013).

In this work, 3D numerical simulation models based on FVM and LBM are applied to predict a dam-break flow propagating through a complex obstacle that represents an idealised city. An experiment was conducted to simulate wave propagations and celerity in an idealized city. The experimental setup consists of an upstream reservoir and four obstacles located at the downstream channel. A dam break flow was observed and recorded by using a high-speed camera. The experimental data are then compared with the numerical simulation results. The FVM and LBM modeling is done by ANSYS Fluent and XFlow commercial software. In both FVM and LBM, the turbulent flow and free surface flow were calculated by using LES and VOF, respectively.

2. Laboratory Experiment

The laboratory experiment was carried out using a rectangular horizontal channel that can be separated to become an upstream reservoir and to place group of four cubic obstacles on the downstream channel. The first case, the four

obstacles were arranged side by side as a 2D array of four with 100 mm separation (Fig. 1). The second case, the four obstacles were separated 85 mm and then rotate 45-degree CCW with respect to the wave front. Therefore, the four obstacles are arranged in two configurations to increase complexity and to change the direction of main flow in a downstream channel, which is referred to as square- and diagonal configuration respectively, as shown in Figure 2a and 2b. A dam-break event is represented by a sudden removal of a vertical plate. Initial condition for water depth in the reservoir is 150 mm. The plate is located at the longitudinal center of the channel and represents the dam gate. For dam-break flow at laboratory experiment, a removal mechanism is constructed to be able to remove the vertical plate instantaneously as shown in Figure 1. A steel rope is connected to the plate top, which is drawn over a pulley with a 10 kg-mass hanging at the other end. By releasing the weight, the plate can be removed.

In the initial test, the upstream reservoir was filled with colorized water. The downstream channel was dried carefully to achieve the dry-bed condition. In the first and second case, a group of four cube obstacles were placed in the downstream channel. A high-speed camera set to 240 frames per second was used and the event was captured from the top view. Flow propagation regimes were observed and it was found that the flow was fully developed in 2 s.
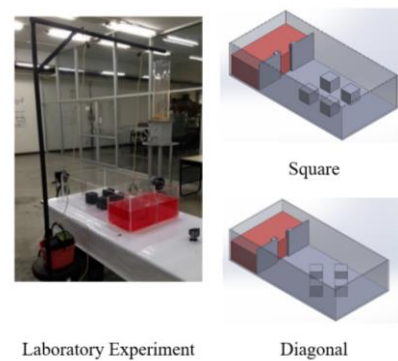

Figure 1. Laboratory experiment of Mechanical Engineering Department, Thammasat University.
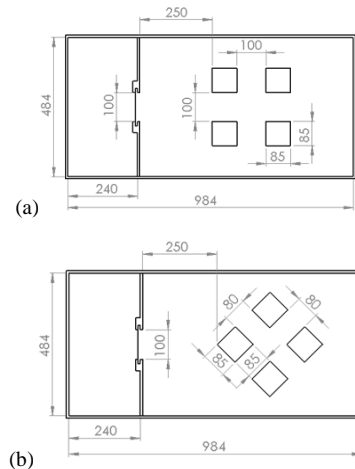

Figure 2. Experiment configurations: (a) square and (b) diagonal (Units: mm).

3. Numerical Models

The novel aspect of the paper was benchmarked for the performance of numerical simulation models based on the Finite Volume Method (FVM) and the Lattice Boltzmann Method (LBM) to capture the free surface flow. Two approaches are adopted by using commercial CFD software, the FVM by ANSYS Fluent software, and the LBM by XFlow software, respectively. The governing equations are described as follows in next section.

3.1 Finite volume method

The finite volume method (FVM) is a discretization method for representing and evaluating partial differential equations in the form of algebraic equations. In this work, the LES and VOF model are used to capture both the shallow water flow and for detailed three-dimensional simulation. In the CFD code, the filtered equations, which express conservation of mass and momentum, can be written by using conservative form given by

$$\frac{\partial \alpha \overline{u}_i}{\partial x_i} = 0 , \tag{1}$$

$$\frac{\partial (\rho \overline{u}_i)}{\partial t} + \frac{\partial (\rho \overline{u}_i \overline{u}_j)}{\partial x_j} = -\frac{\partial \overline{p}}{\partial x_j} + \mu \frac{\partial^2 \overline{u}_j}{\partial x_j^2} + \rho g + \frac{\partial \tau_{ij}^r}{\partial x_j} + F_{vol}, \tag{2}$$

where $\overline{u}_i$ is the filtered resolved quantity in the ith direction [m/s], $\overline{p}$ represents the filtered pressure [Pa], and τ_{ij}^r is the residual stress tensor [s⁻¹]. Closure of the problems is achieved using static Smagorinsky model

$$\tau_{ij}^r = -2 v_t \overline{S}_{ij} , \tag{3}$$

where $\overline{S}_{ij}$ is the rate-of-strain tensor [s⁻¹] for the resolved scale defined by

$$\overline{S}_{ij} \equiv \frac{1}{2} \left(\frac{\partial \overline{u}_i}{\partial x_j} + \frac{\partial \overline{u}_j}{\partial x_i} \right), \tag{4}$$

and v_t is the sub-grid eddy viscosity [m²/s] given by

$$v_t = l_S^2 S = (C_S \Delta)^2 S , \tag{5}$$

where l_s is the mixing length for sub-grid scales [m], C_S is the Smagorinsky coefficient, Δ is computed according to the volume of the computational cells, and S is the strain-rate tensor given by $\sqrt{2} |S_{ij}|$. The C_S value is about 0.1 as the default in ANSYS Fluent.

The VOF model proposed for tracking the gas-liquid interface is achieved by solving the continuity equation for the volume (α) of the two fluid phases. Hence for the qth phase, the continuity equation has the following form

$$\frac{\partial \alpha_q \rho_q}{\partial t} + (\nabla \cdot \alpha_q \rho_q u) = 0 , \tag{6}$$

where u is velocity [m/s]. By knowing the density ρ [kg/m³] and the viscosity μ [Pa.s] of fluid, Equation (6) can be reduced to

$$(\nabla \cdot \alpha_q u) = 0 . \tag{7}$$

The volume fraction equation is solved only for the secondary liquid phase, while the phase fraction of the primary gas is calculated as follows

$$\sum_{q=1}^{n} \alpha_q = 1 . \tag{8}$$

The momentum equation is given by

$$\rho \left(\frac{\partial u_i}{\partial t} + u(\nabla \cdot u) \right) = -\nabla p + \mu \nabla^2 u + \rho g + F_{vol}, \tag{9}$$

where p is pressure [Pa], g and F_{vol} are gravitational acceleration [m/s²] and volume force [N], respectively. Continuum surface force (CSF) is used to simulate surface tension of fluid [N/m]. F_{vol} is the source term of multi-phase flow in the momentum equation as defined by

$$F_{vol} = \sigma_{ij} \frac{\rho k_i \nabla \alpha_i}{0.5 (\rho_i + \rho_j)}, \tag{10}$$

where subscripts i and j denote volume of phases (air and water), σ is the surface tension coefficient, k is the curvature defined by the divergence of the unit normal $\hat{n}$. The relation between the parameters are given by

$$k = \nabla \cdot \hat{n} , \tag{11}$$

where

$$\hat{n} = \frac{n}{|n|} , \tag{12}$$

and

$$n = \nabla \alpha_q . \tag{13}$$

The significance of surface tension was determined by evaluating the Weber number, W_e given by

$$W_e = \frac{\sigma}{\rho_L L U^2}, \tag{14}$$

where ρ_L is liquid density [kg/m³]. U is the free-stream velocity [m/s] and L is the clearance under the down comer [m]. $W_e \gg 1$ indicates that the presence of surface tension is significant and should not be neglected.

The governing equations (Equation 1-14) can be solved by using commercial software ANSYS-Fluent. In order to obtain convergent results for the Cartesian cut-cell grid method, the term discretizing schemes are used in PISO algorithm for splitting the relationship between velocity and pressure. The discretization of QUICK schemes and Compressive are used with the implicit scheme for VOF and open channel model with sharp interfaces. The transient formulation is set to bounded second order implicit for setting different time-dependent solution formulations.

3.2 Lattice Boltzmann method

The lattice Boltzmann method (LBM) was originally developed as an improved version of the Lattice Gas Automata (LGA) by removing statistical noise to achieve better Galilean invariance (Mohamad, 2011). This study uses LBM to simulate the movement and interaction of each fluid particle based on statistics or to display averaged particle density distributions by solving a velocity discrete Boltzmann equation. The LBM is a very efficient mean for simulating especially very complex flow geometries up to several million grid points and overcomes many of disadvantages of traditional CFD methods. The particle-based XFlow CFD code uses fully Lagrangian approach based on LBM and LES turbulence models. The LBM-approach of XFlow code combines LES-turbulence model and a free surface VOF-approach that computational setup of complex CAD-model is not an interactive mesh generation (Maier, 2013). Boltzmann transport equation is defined by

$$\frac{\partial f_i}{\partial t} + e_i \cdot \nabla f_i = \Omega_i, \quad i = 1, ..., b,$$ (15)

where f_i is the particle distribution function in the direction i, e_i is the corresponding discrete velocity and Ω_i is the collision operator.

In the most common approach, Bhatnagar-Gross-Krook (BGK) approximation is introduced as a single-relaxation time τ,

$$\Omega_i^{BGK} = \frac{1}{\tau}\left(f_i^{eq} - f_i\right),$$ (16)

$$v = c_s^2\left(\tau - \frac{1}{2}\right),$$ (17)

and

$$f_i^{eq} = \rho w_i \left(1 + \frac{e_{i\alpha}u_\alpha}{c_s^2} + \frac{u_\alpha u_\beta}{2c_s^2}\left(\frac{e_{i\alpha}e_{i\beta}}{2_s^2} - \delta_{\alpha\beta}\right)\right),$$ (18)

where c_s is the speed of sound [m/s], u is the macroscopic velocity [m/s], δ is the Kronecker delta and w_i are weighting constants built to preserve the isotropy. The α and β are sub-indexes which the different spatial components of the vectors appearing in the equation and Einstein's summation convention over repeated indices has been used.

At low Mach numbers, the single-relaxation time can be used. However, it is not suitable at high Mach number when it causes numerical instabilities (Holman, Brionnaud, & Abiza, 2012). For this reason, the multiple-relaxation-time (MRT) is used instead as the collision operator in XFlow software;

$$\Omega_i^{MRT} = M_{ij}^{-1}\hat{S}_{ij}\left(m_i^{eq} - m_i\right),$$ (19)

where the collision matrix $\hat{S}_{ij}$ is diagonal, m_i^{eq} is the equilibrium value of the moment, m_i and M_{ij} are the transformation matrix. Raw moments are defined as

$$\mu x^k y^l z^m = \sum_i^N f_i e_{iy}^k e_{iy}^l e_{iz}^m$$ (20)

and the central moments is defined as

$$\tilde{\mu} x^k y^l z^m = \sum_i^N f_i \left(e_{ix} - u_x\right)^k \left(e_{iy} - u_y\right)^l \left(e_{iz} - u_z\right)^m.$$ (21)

LBM as a turbulence model can be used by direct numerical simulation or in combination with the Large Eddy Simulation (Chen, 2009). The Smagorinsky constant (C_S) is fixed at 0.1 in this study.

4. Computational Domain, Boundary Conditions and Grids

According to the laboratory experiment, the enclosure (Figure 2a and 2b) was constructed by using 8 mm thickness acrylic. Therefore, computational domains are only fluid volume with 984 mm in length, 484 mm in width, and 200 mm in height. Finite volume mesh is divided by grid cells into fluid domains and the lattice Boltzmann mesh must be determined by using lattice grid spacing.

In order to represent the actual flow, the boundary conditions must be carefully defined. The side and channel bottom walls are adopted by wall boundary condition. An open boundary condition is applied to the top of domain. All surfaces of the channel and obstacles are assumed to be smooth. Therefore, the non-slip boundary condition is defined as zero tangential and normal velocities. A constant volume of fluid with dimensions of 240×484×150 mm representing the reservoir is assigned as the initial condition.

In this work, Cartesian cut-cell grid is used to obtain mesh independence and capture free surface by ANSYS Meshing. This method uses same uniform grid spacing everywhere in the domain, which was varied in such a way that $\Delta x = \Delta y = \Delta z = 8, 6, 5$, and 4 mm, respectively. The same grid spacing is defined in XFlow. The numerical simulations were conducted using 2x Intel Xeon processors x5660 2.8 GHs (12 core 24 threads) and 48 GB of ECC-RAM, which use 8 cores per case.

5. Results and Discussion

In order to keep the speed of sound constant on all grids everywhere in the computational domain, the importance parameters are grid size (Δx) and time-step size (Δt). For the first case, Table 1 shown comparison of the computational time of 4 different grid sizes where flow duration is about $t =$ 2 s. The effect of grid spacing of two numerical models of LBM and FVM are compared by using wall clock time(s). XFlow calculates faster than ANSYS Fluent about 5.96 of wall clock time proportion that is averaged by 4 grid levels. The accuracy of these grids is comparable as can be seen in Figures 3a and 3b, if the same uniform grid spacing is used everywhere in the domain. The comparison of the results of numerical simulation for the 4 different meshes can be shown by free surface at flow time = 0.5 s in which the propagating flow encounters the wall end. The thin layers of water appear near by the dam abutment and wave fronts are captured by smaller grid sizes. The grid 5 mm of LBM (XFlow) can capture better than all simulations of FVM (ANSYS Fluent). Therefore, the grid spacing = 5 mm is used for both ANSYS Fluent and XFlow to predict dam brake flow of two configurations and to compare with experiment data.
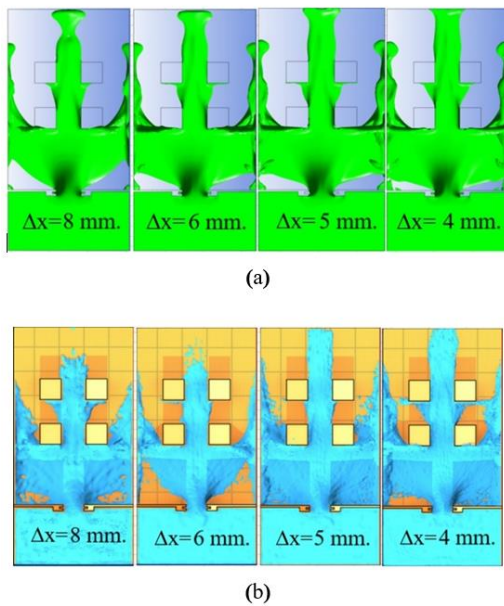

(a)

(b)

Figure 3. Comparison of numerical simulation of free surface fractions of 4 different meshes at time = 0.5 s: (a) Fluent and (b) XFlow.

In the first case, Figure 4 shows a comparison between the experimental and simulation results in case of dam break flow propagation passed through obstacles with the square configuration. The flood wave immediately propagated from upstream reservoir to downstream channel when the dam gate was removed. It was observed that the wave front arrived the obstacles for the first time at time about 0.2 s approximately. Next, the first wave front arrived the following row of obstacles at about time about 0.3 s. After that, the main flow encounters the wall-end at time about 0.5 s. In addition, some parts still develop to the side channel and impact the wall end at time about 0.7 s. Finally, water depth in the downstream channel was increased until same level as the upstream reservoir at time about 0.7-1.2 s.

In the second case, figure 5 shows a flow scenario when four obstacles were arranged in a diagonal confi-guration. When the dam gate removed the first wave front encounters the first obstacle at a time of about 0.2 s. Next time about 0.3 s, wave front was separated by first obstacle and flow arrived the following row of obstacles. Then at the time about 0.4 s and 0.5 s, wave front was separated by following row of obstacles and flow arrived the last obstacle. After that at the time about 0.6 s, the wave front was separated by last obstacle to the side channel and wall-end at the time about 0.7 s. Finally, the depth of the in the downstream area increased until reaching the same level as the upstream reservoir, which makes the two cases similar at time about 0.7-1.2 s. By comparing the flow propagation between simulation results and experimental data of the two cases, it was found that the wave front celerity was slightly slower than experimental results.

The experimental results from high-speed camera in photo format can be fitted to get x-y data of wave front profiles. Figure 6a and 6b show the comparison between experimental and two numerical simulation results of wave front propagating profiles at time about 0.2 s after the dam break. The numerical simulations tend to be more widely and slowly of wave front profiles and celerities than experimental data. For numerical simulation results, LBM results were closer to the experimental data than FVM. Furthermore, figure 7a and 7b show an overall comparison of experimental and two numerical simulation results of maximum wave front celerities at time about 0.1 s, 0.2 s, 0.3 s and 0.4 s respectively. The two numerical simulation results show that the maximum travel is slightly slower than experimental data. It was found in the first case that the FVM and LBM were slower than experiment average of about 38 mm and 35 mm (12.33% and 11%) respectively. In the second case, it was found that the FVM and LBM were slower than experiment

Table 1. Comparison of computational time of 4 different meshes for flow time 2 s.

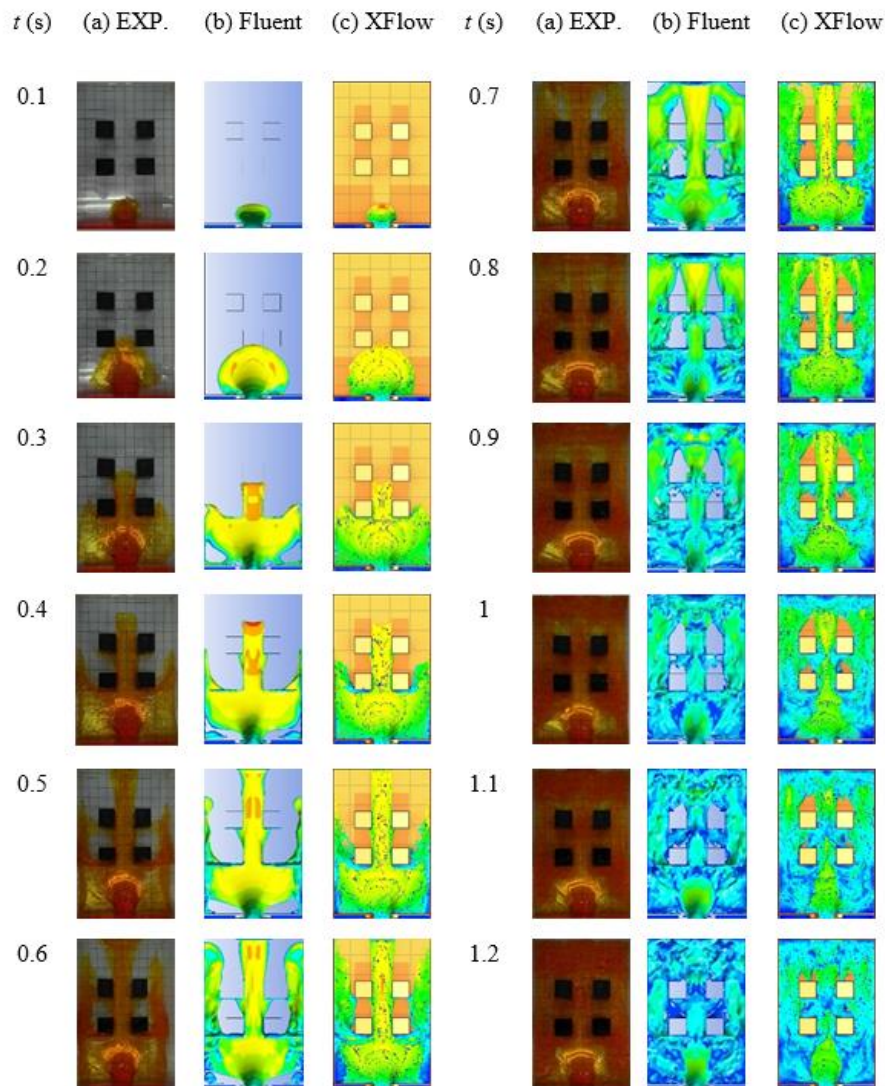| Δx (mm)	Fluent (FVM)		XFlow (LBM)		Time proportion
	meshes	Wall clock time (s)	meshes	Wall clock time (s)	
8	189456	5654.653	173648	723.611	7.81
6	436698	13053.227	435576	2237.101	5.83
5	753821	20243.075	714117	3912.022	5.17
4	1467837	37365.556	1406040	7449.688	5.02
				Average	5.96
				SD.	1.28

Figure 4.   Comparison of (a) Experiment, (b) Fluent, (c) XFlow: with obstacles placed square relative to the flow direction.

average about 17 mm and 25 mm (7.03% and 8.15%), respectively.

6. Conclusions

This paper presents the use of FVM and LBM to predict dam break flow through complex obstacles and to compare the simulation results with experiment. The laboratory experiment was separated and then became an upstream reservoir and the downstream channel and to place four obstacles with two configurations consist of square and diagonal. A high-speed camera set to 240 frames per second was used to capture the photo to observe wave-front propagations and celerities from above. The 3D numerical simulations are modelled by Finite-volume and Lattice Boltzmann methods based on XFlow and ANSYS Fluent. The turbulence flow of the two numerical models is calculated by using Large Eddy Simulation (LES) with the Smagorinsky-Lilly model coupling with Volume of Fluid (VOF) model to tracking the free surface flow.

A comparison of the results shows the computational time of two numerical models with different grid spacing. It is clearly seen that thin layers of water can be illustrated by introducing smaller grid size; however, computational time was increased. When considering thin water captured at dam abutments, the grid spacing 5 mm of XFlow can capture better than all simulations of ANSYS Fluent. ANSYS Fluent and XFlow results provide the minimal difference in the calculation of wave front propagation and celerities, which shows good tendency with experimental data. The resulting mean relative error in the numerical models is less than 12.33% (first case) and 8.15% (second case) when compared to the experimental data but LBM requires less computational time.
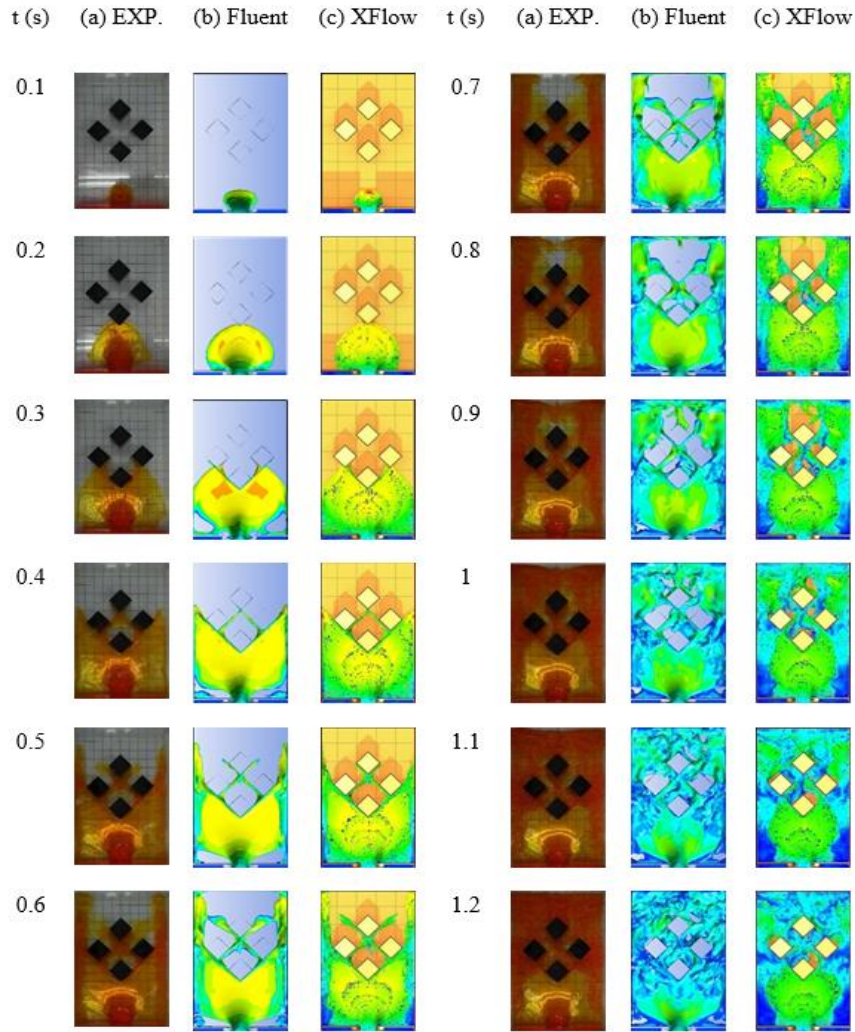
Figure 5.   Comparison of (a) Experiment, (b) Fluent, (c) XFlow: with obstacles placed diagonal relative to the flow direction.
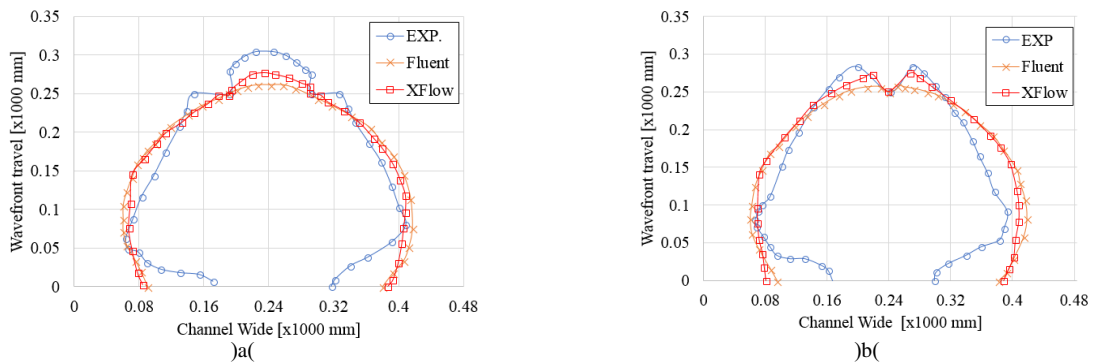

Figure 6.   Comparison of experimental and numerical simulation wave front profiles at time = 0.2 s after the break: (a) Square and (b) Diagonal.

Acknowledgements

References

Albano, R., Sole, A., Mirauda, D., & Adamowski, J. (2016). Modelling large floating bodies in urban area flash-floods via a Smoothed Particle Hydrodynamics model. *Journal of Hydrology*, *541*, 344-358.
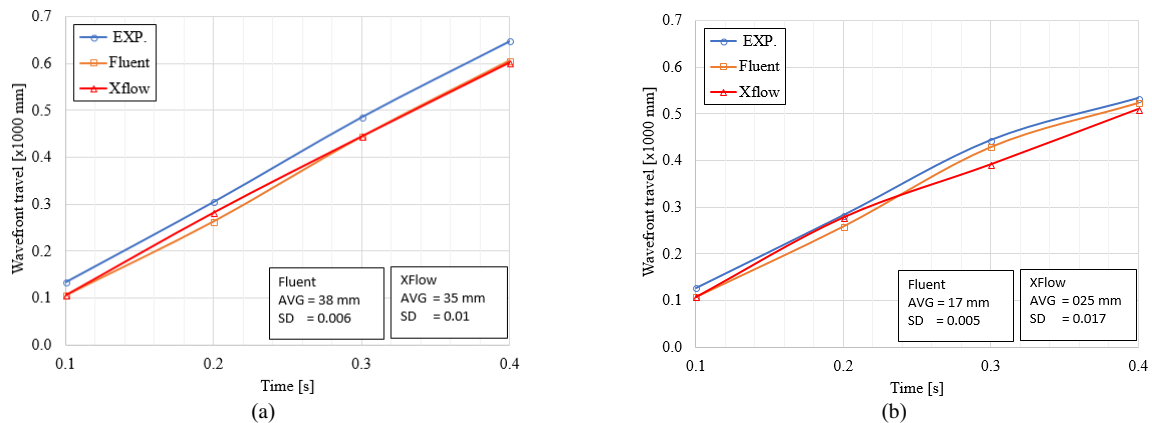
Figure 7. Comparison of experimental and numerical simulations of maximum wave fronts travel at t = 0.1 s, 0.2 s, 0.3 s, and 0.4 s: (a) Square and (b) Diagonal.

Alhasan, Z., Jandora, J., & Říha, J. (2015). Study of dam-break due to overtopping of four small dams in the Czech Republic. *Acta Universitatis Agriculturae et Silviculturae Mendelianae Brunensis*, *63*(3), 717-729.

Biscarini, C., Francesco, S. D., & Manciola, P. (2010). CFD modelling approach for dam break flow studies. *Hydrology and Earth System Sciences*, *14*(4), 705-718.

Biscarini, C., Di Francesco, S., Nardi, F., & Manciola, P. (2013). Detailed simulation of complex hydraulic problems with macroscopic and mesoscopic mathematical methods. *Mathematical Problems in Engineering*, *2013*.

Chen, S. (2009). A large-eddy-based lattice Boltzmann model for turbulent flow simulation. *Applied mathematics and computation*, *215*(2), 591-598.

Di Cristo, C., Evangelista, S., Greco, M., Iervolino, M., Leopardi, A., & Vacca, A. (2018). Dam-break waves over an erodible embankment: experiments and simulations. *Journal of Hydraulic Research, 56*(2), 196-210.

Dickenson, P. (2009). The feasibility of smoothed particle hydrodynamics for multiphase oilfield systems. *Proceeding of Seventh International Conference on CFD in the Minerals and Process Industries*. Melbourne, Australia: CSIRO,

Evangelista, S., Altinakar, M. S., Di Cristo, C., & Leopardi, A. (2013). Simulation of dam-break waves on movable beds using a multi-stage centered scheme. *International Journal of Sediment Research, 28*(3), 269-284.

Evangelista, S. (2015). Experiments and numerical simulations of dike erosion due to a wave impact. *Water*, *7*(10), 5831-5848.

Evangelista, S., Giovinco, G., & Kocaman, S. (2017). A multi-parameter calibration method for the numerical simulation of morphodynamic problems. *Journal of Hydrology and Hydromechanics*, *65*(2), 175-182.

Evangelista, S., Greco, M., Iervolino, M., Leopardi, A., & Vacca, A. (2015). A new algorithm for bank-failure

mechanisms in 2D morphodynamic models with unstructured grids. *International Journal of Sediment Research*, *30*(4), 382-391.

Frazão, S. S., Noël, B., & Zech, Y. (2004, June). Experiments of dam-break flow in the presence of obstacles. *Proceedings of River Flow 2004 Conference, Naples, Italy* (Vol. 2, pp. 911-918).

Hirt, C. W., & Nichols, B. D. (1981). Volume of fluid (VOF) method for the dynamics of free boundaries. *Journal of Computational Physics*, *39*(1), 201-225.

Holman, D. M., Brionnaud, R. M., & Abiza, Z. (2012, September). Solution to industry benchmark problems with the lattice-Boltzmann code XFlow. *Proceeding in the European Congress on Computational Methods in Applied Sciences and Engineering (ECCOMAS)*.

IMPACT. (2004). Investigation of Extreme Flood Processes & Uncertainty (IMPACT), (December), 1–26. Retrieved from www.impact-project.net.

Jian, W., Liang, D., Shao, S., Chen, R., & Yang, K. (2016). Smoothed Particle Hydrodynamics simulations of dam-break flows around movable structures. *International Journal of Offshore and Polar Engineering*, *26*(01), 33-40.

Kajzer, A., Pozorski, J., & Szewc, K. (2014). Large-eddy simulations of 3D Taylor-Green vortex: Comparison of smoothed particle hydrodynamics, lattice Boltzmann and finite volume methods. *Journal of Physics: Conference Series* (Vol. 530, No. 1, p. 012019).

Kao, H. M., & Chang, T. J. (2012). Numerical modeling of dambreak-induced flood and inundation using smoothed particle hydrodynamics. *Journal of Hydrology*, *448*, 232-244.

LaRocque, L. A., Imran, J., & Chaudhry, M. H. (2012). Experimental and numerical investigations of two-dimensional dam-break flows. *Journal of Hydraulic Engineering*, *139*(6), 569-579.

Liu, M. B., & Liu, G. R. (2010). Smoothed particle hydrodynamics (SPH): An overview and recent developments. *Archives of Computational Methods in Engineering*, *17*(1), 25-76.

Maier, H. (2013). *Detailed Flow Modelling of Mixing Tanks based on the Lattice Boltzmann Approach in XFlow*. Madrid, Spain.

Marsooli, R., & Wu, W. (2014). 3-D finite-volume model of dam-break flow over uneven beds based on VOF method. *Advances in Water Resources*, *70*, 104-117.

Mohamad, A. A. (2011). *Lattice Boltzmann method: fundamentals and engineering applications with computer codes*. Berlin, Germany: Springer.

Monaghan, J. J. (1992). Smoothed particle hydrodynamics. *Annual Review of Astronomy and Astrophysics*, *30*(1), 543-574.

Morris, M. (Ed.). (1999). *Concerted Action on Dam-break Modelling: Proceedings of the CADAM Meeting, Wallingford, United Kingdom, 2-3 March 1998*. Brussels, Belgium: Office for Official Publications of European Communities.

Onda, S., Hosoda, T., Jaćimović, N. M., & Kimura, I. (2018). Numerical modelling of simultaneous overtopping and seepage flows with application to dike breaching. *Journal of Hydraulic Research*, 1-13.

Robb, D. M., & Vasquez, J. A. NUMERICAL Simulation of dam-break flows using depth-averaged hydrodynamic and three-dimensional cfd models. *Proceeding of Canadian Society for Civil Engineering 22nd Hydrotechnical Conference.*Soares-Frazão, S., & Zech, Y. (2007). Experimental study of dam-break flow against an isolated obstacle. *Journal of Hydraulic Research*, *45*(Suppl. 1), 27-36.

Soares-Frazão, S., & Zech, Y. (2008). Dam-break flow through an idealised city. *Journal of Hydraulic Research*, *46*(5), 648-658.

Syvitski, J. P., Slingerland, R. L., Burgess, P., Meiburg, E., Murray, A. B., Wiberg, P., ... & Voinov, A. A. (2009). Morphodynamic models: An overview. *River, Coastal and Estuarine Morphodynamics, RCEM*, 3-20.

Tayfur, G., & Guney, M. (2013). A physical model to study dam failure flood propagation. *Water Utility Journal*, *6*, 19-27.

Xu, K., & He, X. (2003). Lattice Boltzmann method and gas-kinetic BGK scheme in the low-Mach number viscous flow simulations. *Journal of Computational Physics*, *190*(1), 100-117.

Xu, X. (2016). An improved SPH approach for simulating 3D dam-break flows with breaking waves. *Computer Methods in Applied Mechanics and Engineering*, *311*, 723-742.

Yang, C., Lin, B., Jiang, C., & Liu, Y. (2010). Predicting near-field dam-break flow and impact force using a 3D model. *Journal of Hydraulic Research*, *48*(6), 784-792.